Journal of Tropical Resources and Sustainable Science
Website : http://journal.umk.edu.my/index.php/jtrss/
eISSN : 2462-2389
Vol: SI Issue 1, 2025, 134-143
DOI: https://doi.org/10.47253/jtrss.v13i3.2010

RESEARCH ARTICLE

Evaluation of groundwater sources using Electrical Resistivity Imaging (ERI) method in Felda Tersang 02, Raub, Pahang

Noorzamzarina Sulaiman[1,2*], Nur Iman Farhana Rafii[1], Nursufiah Sulaiman[1,2] and Fazrul Razman Sulaiman[3]

[1]Geoscience Department, Faculty of Earth Science, Universiti Malaysia Kelantan Jeli Campus, 17600 Jeli, Kelantan, Malaysia.
[2]Tropical GeoResources & Hazards Research Group, Faculty of Earth Science, Universiti Malaysia Kelantan Jeli Campus, 17600 Jeli, Kelantan, Malaysia.
[3]Faculty of Applied Sciences, Universiti Teknologi MARA (UiTM) Cawangan Pahang, 26400 Bandar Tun Abdul Razak Jengka, Pahang, Malaysia.

ARTICLE HISTORY
Received : 22 July 2025
Accepted : 26 October 2025
Online : 31 December 2025

KEYWORDS
groundwater sources,
Electrical Resistivity Imaging (ERI),
Schlumberger array configuration,
2D pseudosection,
Res2Dinv software.

☒ * **CORRESPONDING AUTHOR**
Noorzamzarina Sulaiman
Geoscience Department, Faculty of Earth Science, Universiti Malaysia Kelantan Jeli Campus, 17600 Jeli, Kelantan, Malaysia
Email: zamzarina@umk.edu.my

ABSTRACT

This study employed the Electrical Resistivity Imaging (ERI) technique in the Felda Tersang 02 area of Raub, Pahang, to address the region's water supply issues. The study area is primarily composed of sandstone, slate, and dacite. Groundwater, critical for sustaining agricultural and industrial demands, is rapidly depleting due to unsustainable extraction. However, since the underlying geology and hydrogeology are complex, investigating and assessing groundwater sources can be challenging. By measuring the electrical resistivity of underlying materials, a geophysical technique called Electrical Resistivity Imaging (ERI) is used to map and evaluate groundwater sources. Each survey line is 200 m long with 41 takeouts spaced 5 m apart, using the Schlumberger and pole-dipole configurations. The study's findings will aid with groundwater resource management and provide a deeper understanding of the region's subsurface geology and hydrogeology. The 2D pseudosection results for all three survey lines reveal a significant accumulation of groundwater in a large geographical area. The identified low-resistivity range (0–100 Ωm) serves as a significant indicator of water-bearing formations, providing valuable insights into the area's groundwater potential.

1. INTRODUCTION

The growing pressure on groundwater resources, driven by rapid population growth, industrial development, and agricultural expansion, has created a critical need for effective and efficient groundwater management strategies (Soekarno et al., 2024; Petrick et al., 2023). As freshwater resources become increasingly scarce and surface water bodies continue to deteriorate in quality, reliance on subsurface water has intensified. Consequently, interest in groundwater exploration has expanded significantly to meet the escalating water demand (Suryadi et al., 2019). Pollution, urbanization, and climate variability further compound this growing dependence on underground water, exerting additional stress on aquifer systems and threatening the sustainability of groundwater supplies. Hence, the increasing challenges compel hydrogeologists and water resource managers to adopt innovative and integrated approaches that provide both spatial and temporal information on groundwater systems for sustainable management and protection.

Electrical Resistivity Imaging (ERI) has emerged as one of the most powerful and widely adopted geophysical techniques for groundwater exploration and environmental investigations. The method offers a reliable means of examining subsurface characteristics by measuring the variation in electrical resistivity of geological materials. It allows for detailed analysis of soil and rock properties, stratification, and subsurface heterogeneities, as well as the identification of cavities, fractures, and saturated zones that exhibit distinct physical contrasts relative to their geological surroundings (Dor et al., 2011). Numerous studies have demonstrated that ERI is among the most effective and versatile non-invasive geophysical methods for groundwater assessment and environmental studies (Azhar et al., 2016; Saad et al., 2012). ERI's ability to map lithological variations and delineate potential water-bearing zones enables it to serve as an indirect indicator of groundwater distribution and quality. It can detect areas of varying salinity or clay content, which are essential for identifying aquifer boundaries and contamination zones. This is particularly advantageous in

tropical regions such as Malaysia, where deep weathering profiles, heterogeneous soil layers, and fractured bedrock often create strong resistivity contrasts that can be effectively visualized through ERI surveys. For instance, Abdul Nassir et al. (2000) successfully applied resistivity imaging to delineate groundwater aquifer boundaries, distinguishing between clay and sand layers, and differentiating between fresh and saline groundwater zones. A key advantage of ERI lies in its non-invasive and eco-friendly nature, minimizing environmental disturbance while yielding critical subsurface data (Adeeko & Nordiana, 2018).

According to Acworth (2001), ERI provides an invaluable non-destructive means of obtaining subsurface information essential for hydrological assessments. The technique enables the visualization of underground structures without the need for extensive drilling, thereby reducing both costs and ecological impact. By allowing the visualization of aquifer geometry, ERI enhances understanding of groundwater flow systems, recharge zones, and potential contamination pathways. Its ability to characterize layered media based on resistivity contrasts has made it standard practice in hydrogeological surveys over the past several decades. Moreover, ERI's sustainability stems from its minimal site disturbance, low operational impact, and ability to complement traditional hydrogeological and drilling data (Azhar et al., 2016).

ERI is particularly effective in delineating aquifer boundaries, identifying contamination-prone zones, and mapping hydrogeological features in complex terrains (Rajendran et al., 2020; Oyeyemi et al., 2018). In heterogeneous environments where lithological variability is high, conventional methods such as borehole drilling often provide limited spatial coverage and can be prohibitively expensive. ERI, on the other hand, offers continuous subsurface imaging, allowing for the identification of subtle variations in lithology, porosity, and moisture content that might otherwise go undetected. For example, Vaudelet et al. (2011) demonstrated the technique's effectiveness in mapping oil contamination within aquifers, clearly illustrating pollutant dispersion patterns relative to geological structures. This exemplifies how ERI can be employed not only in freshwater exploration but also in environmental monitoring and contamination studies, enhancing its versatility and scope of application.

The high-resolution imaging capability of ERI enables detailed visualization of subsurface features, facilitating the mapping of groundwater reservoirs, aquifer boundaries, and recharge areas while also identifying potential pollution pathways. This resolution is particularly beneficial for evaluating groundwater salinity gradients in coastal regions, where saltwater intrusion poses significant risks to freshwater supplies (Galazoulas et al., 2015). Similarly, Batayneh (2006) demonstrated ERI's success in semi-arid environments by distinguishing resistivity variations associated with lithological differences and saturation levels, further confirming its reliability in diverse hydrogeological settings. Such applications demonstrate ERI's sensitivity in detecting both vertical and lateral resistivity changes, making it an indispensable technique for characterizing complex aquifer systems.

Given its adaptability, precision, and environmental compatibility, ERI represents a cornerstone in modern groundwater exploration and management. Its integration into groundwater studies enables researchers and policymakers to make informed decisions regarding water resource sustainability, land-use planning, and the mitigation of contamination. By providing a clear depiction of subsurface structures, ERI supports the identification of productive aquifers, monitoring of groundwater recharge, and assessment of pollution risks. Furthermore, when coupled with other hydrological and geological data, ERI contributes to the development of comprehensive groundwater management frameworks that support long-term environmental resilience.

Therefore, this study aims to assess the groundwater potential in Felda Tersang 02 using the Electrical Resistivity Imaging (ERI) method, providing valuable insights into the subsurface characteristics, aquifer distribution, and overall groundwater potential of the area. The integration of ERI data with geological and hydrological analyses will help to enhance the understanding of groundwater systems in the study area, contributing to sustainable water resource development and informed environmental management.

2. MATERIALS AND METHODS

2.1. Study area

This study area is located at Felda Tersang 02, Raub, Pahang, which lies within the central region of Peninsular Malaysia. The surveyed area encompasses approximately 25 km² (5 x 5 km) and represents a geologically and geomorphologically diverse terrain. Figure 1 illustrates the basemap of the study area, highlighting the spatial extent of the investigation and the key geological units present. The area is renowned for its intricate geological framework, which encapsulates a significant portion of the tectonic and mineralization history of the Raub District. This complexity makes Felda Tersang 02 an ideal location for hydrogeological and geophysical investigations, particularly in relation to groundwater resource assessment and mineral exploration.

The Bentong–Raub Suture Zone (BRSZ) forms the most prominent geological feature within this region and serves as a significant structural boundary dividing two major geological provinces of the Malay Peninsula—the Central Belt and the Eastern Belt (Khan and Shuib, 2016). This suture zone represents a remnant of an ancient oceanic crust that once separated two continental blocks, namely the Sibumasu and Sunda terranes. The convergence and eventual collision of these terranes during the Late Paleozoic to Early Mesozoic periods (~250–200 Ma) resulted in intense tectonism, regional metamorphism, and crustal deformation. This tectonic event played a pivotal role in shaping the current lithological and structural characteristics of the Raub area.

The Bentong–Raub Suture Zone is characterized by a complex assemblage of metamorphic, sedimentary, and ultramafic rocks, indicating subduction-related processes and continental collision dynamics. The tectonic compression and shearing associated with this event contributed to the formation of fault zones, fractures, and joint systems, which continue to influence the region's hydrogeological and geomorphological patterns. Moreover, these structural features act as conduits for fluid migration and mineralization, facilitating the deposition of economically significant minerals such as gold, arsenopyrite, and pyrite, especially along fault zones and vein systems (Hutchison, 2009). The Raub Gold Belt, which extends through the study area, is one of the most well-known mineralized zones in Malaysia and bears testimony to the area's rich tectono-magmatic evolution.

The study area exhibits four dominant rock types: slate, limestone, sandstone, and volcanic rocks (primarily dacite). These lithological units reflect distinct depositional and volcanic environments over geological time. The slate units, representing the oldest lithology, belong to the Silurian–Ordovician sequence and were originally marine sediments subjected to low-grade regional metamorphism. These slates often occur in thinly bedded, foliated layers and are frequently interbedded with phyllite and shale, indicative of deep marine deposition followed by subsequent tectonic deformation. The limestone units, typically from the Permian period, are characterized by fossiliferous and recrystallized textures, suggesting deposition in a shallow marine carbonate platform. These limestone outcrops occasionally exhibit karstic features due to dissolution processes, which are important in influencing groundwater storage and flow.

The sandstone formations, intercalated with shale and siltstone, denote deltaic to nearshore depositional settings, reflecting a transition from marine to continental conditions. They often display cross-bedding and other sedimentary structures indicative of fluvial and tidal influences. Meanwhile, the volcanic rocks, predominantly dacite of Triassic age, mark a phase of volcanic activity following the closure of the oceanic basin. These rocks are typically porphyritic in texture and may show varying degrees of weathering and alteration. The presence of volcanic materials interbedded with sedimentary units signifies an active tectono-volcanic environment during the Mesozoic period.

The lithological distribution of the area thus reveals a progressive depositional transition from marine and deltaic environments to volcanic settings, consistent with regional geological evolution models (Metcalfe, 2013). The Silurian–Ordovician slates represent the initial deep marine sedimentation, succeeded by Permian shallow marine carbonates, and culminating in Triassic volcanic sequences associated with orogenic uplift and magmatism. This lithostratigraphic succession reflects multiple phases of basin development, sedimentation, deformation, and magmatic intrusion that have collectively shaped the geologic character of Felda Tersang 02.

Geomorphologically, the area displays a diverse landscape, ranging from low to high hills, ridges, and floodplains, each reflecting different stages of tectonic uplift, denudation, and erosion. The highlands, often underlain by resistant volcanic or metamorphic rocks, form steep slopes and rugged terrain, while the low-lying regions comprise weathered sedimentary deposits and alluvial plains. These landforms are intricately controlled by structural lineaments, which direct surface drainage and influence the distribution of weathered materials. Tectonic activities, weathering processes, and fluvial erosion have played dominant roles in shaping the surface morphology. The presence of fault-controlled valleys and dissected hills also highlights the geomorphological impact of the Bentong–Raub suture's reactivation over geological time.

The weathering profile in the study area is typically deep, especially over granitic and volcanic terrains, leading to the formation of residual soils and saprolite layers. These weathered materials, characterized by variable permeability, play a crucial role in controlling groundwater recharge and storage capacity. The hydrogeological potential of the region is closely related to the degree of fracturing and weathering within the rock units, with the slate and sandstone formations generally serving as semi-permeable aquifers, while limestone zones may exhibit high secondary porosity due to karstification.

Overall, the geological and geomorphological setting of Felda Tersang 02 is the product of a long and complex geotectonic evolution, dominated by the influence of the Bentong–Raub Suture Zone. The interplay between ancient depositional environments, magmatic intrusions, and subsequent tectonic deformation has resulted in a highly heterogeneous subsurface characterized by varied rock types

and structural fabrics. This diversity not only underpins the mineralization history of Raub but also provides key insights into the hydrogeological framework that governs groundwater occurrence and movement within the study area.

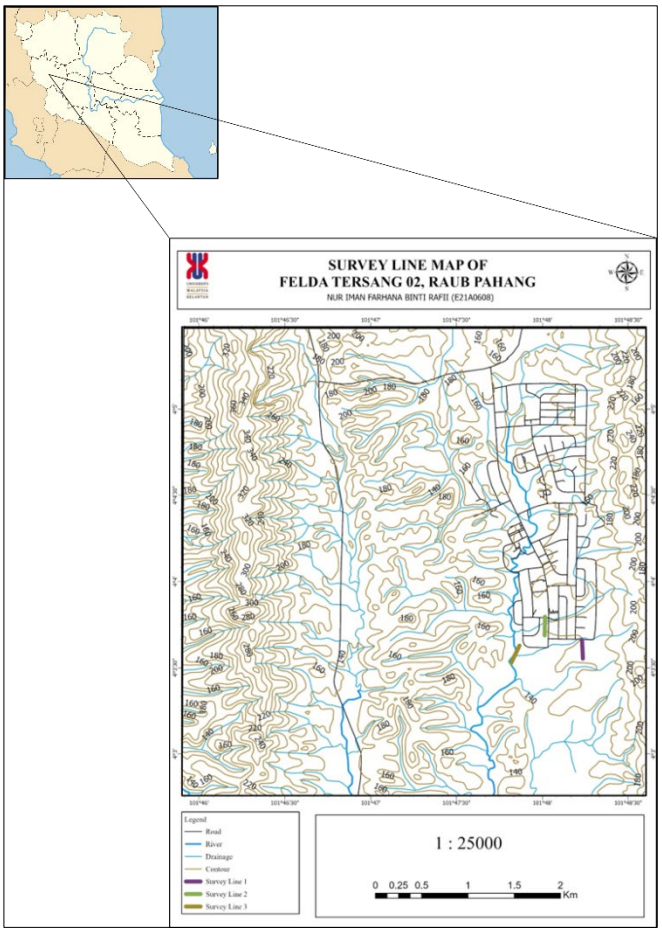

Figure 1: The basemap of study area indicates three survey lines at Felda Tersang 02, Raub, Pahang.

2.2 Methodology

The ABEM Terrameter LS, in conjunction with an electrode selector, was utilized to conduct an electrical resistivity imaging (ERI) survey. Three electrical resistivity profiles were acquired across the chosen study region. The testing design included a Schlumberger and pole-dipole array consisting of two multi-core electrode cables and 41 stainless-steel electrodes. A uniform electrode spacing of five meters was employed across all 41 electrodes, resulting in a total length of the electrical resistivity survey of 200 meters. The survey traverses are aligned in a north to south orientation (spread lines 1, 2, and 3). The Schlumberger array is used for data collection due to its capability to provide high-density coverage of resistivity data in the near-surface region. This array has excellent vertical resolution and can produce distinct images of groundwater and sand-clay borders as horizontal structures (Chambers et al., 2014; Samsudin, 2016). Additionally, the Schlumberger array facilitates a more comprehensive analysis of subsurface profiles within a confined area. Schlumberger array is known for its ability to provide high-resolution vertical profiles, which are particularly effective in delimiting lithological layers and aquifers (Ejije & Atakpo, 2025). Conversely, the network of poles-dipoles is known for its extended exploration depth, which makes it well-suited for studying larger geological formations (Akhtar et al., 2021).

Employing the Res2DInv software, the pole-dipole array technique was used to gather data and generate resistivity images for modeling and result interpretation (Loke et al., 2006; Abdullah et al., 2022). The non-unification and ambiguity inherent in resistivity data require a more complicated interpretation. The relationship between the variation of resistivity and underground materials is often non-linear, making it difficult to definitively deduce the geological structures from the values of resistivity (al-Khafaji, 2023). Advanced inversion algorithms and modeling techniques are crucial for addressing these interpretation challenges (Azizan et al., 2018).

The raw data collected from data gathering were initially processed using the commercially available RES2DINVx64 software to generate an inverse model that closely approximates the actual subsurface structure. The RES2DINVx64 inversion algorithm is utilized to process the data and generate a 2-D resistivity section. The raw data is exported into a DAT file during the field data processing (Loke, 2002). To ensure accurate results, it is essential to eliminate any faulty data points before processing. Resisting the removal of the erroneous data points will lead to an imprecise outcome in the final results. Typically, the presence of faulty data points is due to inadequate contact between the electrodes and the ground during data collection in the field. The final product is presented in a pseudosection profile with the fewest possible errors.

3. RESULT AND DISCUSSION

3.1 Survey Line 1

This survey line, oriented along a north–south direction, employs the Schlumberger electrode configuration, which is known for its high sensitivity to vertical variations in subsurface resistivity. The total root-mean-square (RMS) error of 4.0% obtained from the resistivity inversion process indicates that the model fitting is within an acceptable range, suggesting high reliability and accuracy of the acquired data. This low RMS error also reflects the quality of field data acquisition, proper electrode contact resistance, and a robust inversion process with minimal noise interference.

The resistivity and chargeability results obtained from the two-dimensional (2-D) inversion model reveal significant subsurface variations within the upper 35 meters of the profile. In the shallow subsurface (<35 m depth), the resistivity values vary from 0 Ωm to 1300 Ωm, while

chargeability values range between 0.00 ms and 7.00 ms. Figure 2 illustrates the 2-D pseudosection profile, which has been divided into two distinct interpretive zones; Zone A and Zone B, based on the spatial distribution of resistivity and chargeability characteristics.

Zone A is characterized by low resistivity values ranging from 0 Ωm to 100 Ωm, represented by blue to green tones on the pseudosection. These low-resistivity zones generally indicate the presence of conductive materials, such as saturated soils, clayey sediments, or groundwater-bearing formations. In hydrogeophysical interpretation, resistivity values below 80 Ωm are commonly associated with unconsolidated sand or sandy clay layers that possess moderate to high porosity and permeability, thus indicating potential groundwater occurrence (Riwayat et al., 2018). The electrical response of this zone suggests that it may correspond to an aquifer horizon or a water-saturated weathered layer that facilitates groundwater accumulation and movement.

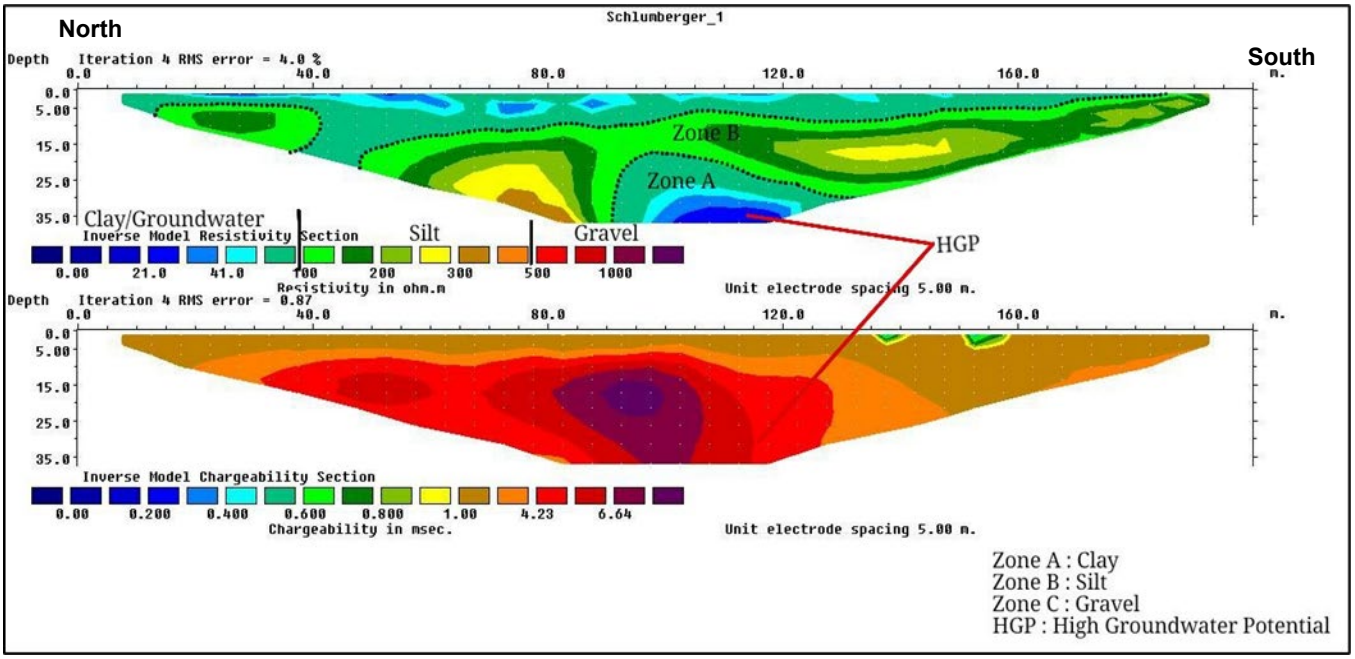

Figure 2: Apparent-resistivity pseudosection (top) and chargeability (bottom) profile of Line 1.

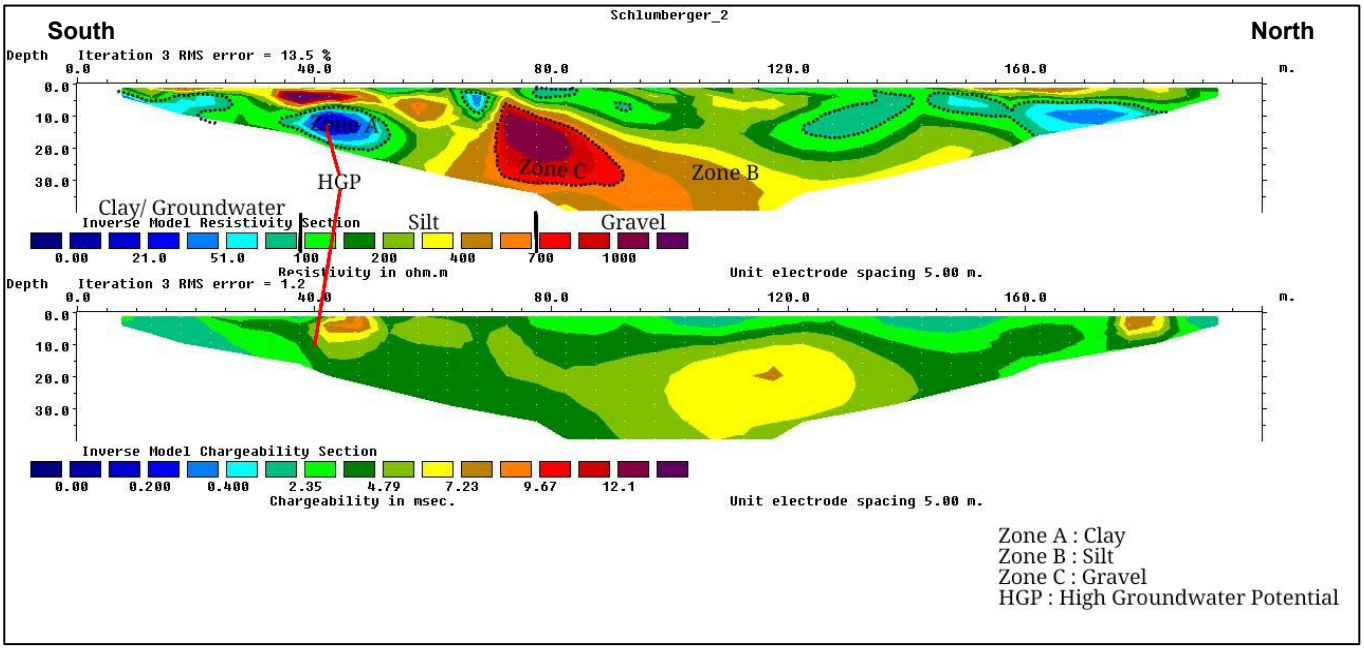

Figure 3: Apparent-resistivity pseudosection (top) and chargeability (bottom) profile of Line 2

Zone B, on the other hand, exhibits moderate resistivity values ranging from 100 Ωm to 500 Ωm, which are represented by green, yellow, light orange, and orange color shades in the pseudosection. These resistivity values typically correspond to residual soils, lateritic materials, or moderately weathered bedrock formations. Such materials may possess

limited groundwater potential depending on the degree of weathering and fracturing. The intermediate resistivity response indicates that the zone might represent a transition between the saturated and unsaturated layers, where partial water saturation or compacted soil textures limit groundwater flow.

The chargeability distribution further complements the resistivity interpretation. High chargeability regions (depicted in orange to red tones) may indicate the presence of clay-rich or mineralized materials, which are known to store charge due to their cation exchange capacity. These materials tend to have lower hydraulic conductivity, which restricts the movement of groundwater. Conversely, areas exhibiting low chargeability values (green to yellow tones) are typically associated with sandy or coarse-grained materials that allow greater permeability, signifying possible groundwater-bearing formations.

Within Zone A, particularly at depths between 20 and 35 meters, an aquifer layer is inferred based on the combination of low resistivity (ranging from 21 Ωm to 100 Ωm) and moderate chargeability (approximately 4.23 ms). This zone demonstrates the characteristics of a saturated formation, likely composed of sand or sandy clay, where groundwater accumulation is significant. The consistency of these results with findings by Noorzamzarina et al. (2024) further validates the interpretation, as they reported that potential groundwater zones within the same study area exhibit resistivity values ranging from of 24.1 Ωm to 100 Ωm.

Overall, the interpretation of the resistivity and chargeability data along this survey line suggests a heterogeneous subsurface with variable lithological and hydrological characteristics. The identified low-resistivity zone in the deeper section of Zone A represents a promising groundwater-bearing layer, while the moderate-resistivity areas in Zone B may indicate partially saturated or weathered bedrock zones with limited groundwater yield. These findings contribute valuable insight into the spatial distribution of subsurface materials and groundwater potential, thereby supporting the broader objectives of hydrogeological assessment and sustainable groundwater resource management in the study area.

3.2 Survey Line 2

This survey line, oriented from south to north, employed the Schlumberger electrode configuration, which is widely recognized for its strong capability in resolving vertical variations in subsurface resistivity while maintaining excellent depth penetration. This configuration is particularly advantageous in groundwater exploration, where identifying vertical changes in lithology and moisture content is crucial for understanding aquifer geometry and groundwater potential (Nugraha et al., 2025). The inversion of the apparent resistivity data produced a root-mean-square (RMS) error of 13.5%, signifying an acceptable level of accuracy and a reliable fit between the measured and modeled datasets. Such an error range suggests that the inversion model provides a trustworthy representation of the true subsurface electrical properties and can thus be confidently used for geological and hydrogeological interpretation.

At depths exceeding 35 m, the resistivity values range between 0 Ωm and 1300 Ωm, while the chargeability values vary from 0.00 ms to 14 ms, indicating a heterogeneous subsurface environment with diverse lithological compositions and varying degrees of water saturation. These wide variations suggest the coexistence of conductive and resistive materials, reflecting a complex interplay between clayey layers, weathered bedrock, and fractured zones that control groundwater occurrence and movement (Nugraha et al., 2025). As illustrated in Figure 3, the resulting 2-D resistivity–chargeability pseudosection is subdivided into three distinct zones—A, B, and C—each characterized by unique electrical and geological features.

Zone A, represented predominantly by blue to light green hues, displays low resistivity values (0–100 Ωm) and low-to-moderate chargeability (~3 ms). These characteristics are typical of highly conductive, water-saturated materials such as alluvial sediments, weathered bedrock, or fractured zones that facilitate groundwater accumulation and movement (As'ari et al., 2024). The low resistivity is attributed to the presence of clayey sand, silt, or fine-grained soils with significant water content, whereas the low chargeability reflects the dominance of pore water conduction rather than the presence of metallic or clay minerals (Revil et al., 2024). This electrical signature strongly suggests the presence of a shallow aquifer system at depths of approximately 5–20 m, making it a potential groundwater-bearing zone suitable for small-scale extraction and community water supply.

Zone B, which appears as green, yellow, and orange tones on the pseudosection, demonstrates moderate resistivity values (100–700 Ωm) and slightly elevated chargeability. These values are indicative of partially saturated or semi-permeable materials, such as sandy clay, silt, or weathered rock, that form transitional hydrogeological layers between permeable aquifers and impermeable bedrock (Noorzamzarina et al., 2024). The moderate resistivity suggests limited water retention capacity, while the increased chargeability implies the presence of mixed lithologies with variable clay content or minor metallic mineralization. Such characteristics are consistent with aquitard behavior, where water movement is restricted but slow percolation may still

occur. Similar intermediate resistivity–chargeability patterns have been documented in humid tropical environments, indicating transitional zones that control recharge and groundwater flow (Javed et al., 2024).

In contrast, Zone C, illustrated by dark red to purple colors, corresponds to high resistivity values (700–1300 Ωm) and negligible chargeability, signifying dense, compact, and dry lithologies such as granite, quartzite, or consolidated bedrock. The absence of significant chargeability response supports the interpretation of impermeable and non-conductive materials, implying poor groundwater potential. This zone likely represents the basement rock or unweathered bedrock layer, forming the hydrogeological boundary that limits further downward percolation of groundwater.

Overall, the 2-D resistivity and chargeability model delineates two major subsurface divisions: (i) a shallow resistive layer (>1000 Ωm) that likely represents a lateritic or weathered crust, and (ii) a deeper conductive layer (10–100 Ωm) associated with clay-rich or water-bearing formations (Noorzamzarina et al., 2023; Islami et al., 2024).

The strong correlation between low resistivity and low chargeability values in the upper layers confirms the presence of porous, water-saturated zones, whereas the combination of moderate-to-high chargeability with intermediate resistivity indicates clay-rich or partially mineralized layers (Revil et al., 2024). This relationship is essential for distinguishing between true aquifer zones and clay-dominated conductive zones, which may otherwise exhibit similar resistivity ranges.

A promising aquifer horizon is inferred within Zone A along Line 2, at depths of 5–20 m, characterized by resistivity values between 21 Ωm and 100 Ωm and chargeability around 3 ms. These geophysical signatures are consistent with productive shallow aquifers identified in previous ERI-based groundwater studies, which reported similar resistivity–chargeability correlations for aquifer delineation and groundwater potential mapping (As'ari et al., 2024; Javed et al., 2024). Hence, this layer represents a key groundwater target zone with potential for sustainable groundwater extraction, contributing valuable insights into groundwater resource management and future borehole sitting in the study area.

3.3 Survey Line 3

Survey Line 3 was conducted using the pole–dipole electrode configuration, oriented from south to north, which effectively captures both lateral and vertical variations in subsurface resistivity and chargeability. This configuration provides a good balance between depth penetration and horizontal resolution, making it particularly useful for delineating heterogeneous subsurface materials in complex geological terrains (Javed et al., 2024). The inversion results yielded a root mean square (RMS) error of 10.8%, signifying a satisfactory correlation between the measured and calculated apparent resistivity values and confirming that the inversion model reliably represents the true subsurface conditions (Nugraha et al., 2025).

At depths exceeding approximately 75 m, resistivity values range from 0 Ωm to 1300 Ωm, while chargeability values vary between 0.00 ms and 12 ms. These broad ranges indicate complex lithological and hydrogeological conditions influenced by variations in mineral composition, degree of weathering, porosity, and groundwater saturation (Revil et al., 2024). Based on the distribution patterns of resistivity and chargeability observed in the pseudosection (Figure 4), the subsurface can be broadly divided into two major zones: Zone B and Zone C, each representing distinct lithological and hydrogeological characteristics.

Zone B is characterized by moderate resistivity values ranging from 100 Ωm to 700 Ωm, represented by green to light red tones on the pseudosection. This range is indicative of weathered or fractured bedrock, silty to clayey materi als, and partially saturated residual soils. The moderate resistivity values suggest the presence of both mineral grains and conductive pore water, typical of zones exhibiting secondary porosity as a result of fracturing and weathering. Within the 20–60 m depth range, chargeability values reach up to 12 ms, reflecting the presence of fine-grained sediments or ion-rich pore fluids that enhance polarization effects. The combined resistivity and chargeability responses indicate a moderately permeable aquifer zone with potential for groundwater infiltration and storage. This interpretation is consistent with weathered bedrock horizons that commonly act as transitional layers between the overburden and unweathered bedrock, providing suitable conditions for groundwater accumulation (Hazreek et al., 2018; Noorzamzarina et al., 2024).

In contrast, Zone C exhibits high resistivity values ranging between 700 Ωm and 1300 Ωm and is represented by dark red to violet hues on the pseudosection. These values correspond to compact, dry, and impermeable lithologies, such as unweathered granite or other crystalline igneous rocks. The low chargeability values recorded in this zone support its interpretation as the unweathered basement, which is typically massive, non-porous, and poorly fractured, resulting in minimal groundwater storage potential. The interface between Zones B and C likely represents a hydrogeological boundary where groundwater flow is either restricted or redirected along fractures and weathered pathways above the bedrock. Such interfaces are important in hard rock aquifers, as they control the movement and

accumulation of groundwater in secondary porosity zones (Nugraha et al., 2025).

The integration of Induced Polarization (IP) data with resistivity analysis enhances the accuracy and reliability of subsurface interpretation. While resistivity primarily reflects variations in lithology and fluid content, chargeability provides additional information related to the electrochemical properties of the subsurface materials, such as clay content, metallic minerals, or the presence of ion-rich fluids (Revil et al., 2024). This complementary relationship between resistivity and chargeability enables a more comprehensive differentiation between resistive (bedrock or dry) and conductive (saturated or clay-rich) zones. The combined use of these datasets strengthens the interpretative framework by providing both structural and compositional information, thus facilitating a more holistic understanding of the hydrogeological setting. Similar conclusions have been drawn by Revil et al. (2024) and Javed et al. (2024), who demonstrated that integrated ERI–IP approaches significantly improve subsurface characterization in geologically complex environments.

Based on the classification scheme proposed by Hazreek et al. (2018) and supported by more recent findings by Noorzamzarina et al. (2024), the subsurface materials along Survey Line 3 can be categorized into three main lithological types: (i) dense or hard soils and unweathered volcanic or igneous rocks, which typically exhibit high resistivity values (>1500 Ωm) and have limited groundwater potential; (ii) permeable to semi-permeable residual soils and weathered formations, which display moderate resistivity values (1–1500 Ωm) and variable saturation levels, representing the primary groundwater-bearing units; and (iii) soft, water-saturated sediments or clay-rich zones, characterized by low resistivity values (<100 Ωm) and high chargeability, indicating high moisture content or the presence of conductive clay minerals. Although the third category is not prominently developed along this line, localized conductive anomalies at shallow depths may correspond to isolated clayey or water-saturated pockets.

Overall, the findings from Survey Line 3 underscore the effectiveness of the Electrical Resistivity Imaging (ERI) technique, particularly when complemented by IP measurements, in identifying subsurface variations and potential groundwater-bearing zones. The integration of resistivity and chargeability data provides a robust interpretative approach that allows for differentiation between dry and saturated formations, delineation of weathered and fractured bedrock, and identification of potential aquifer zones. This integrated interpretation enhances the understanding of the geological and hydrogeological framework of the study area, contributing valuable insights for groundwater assessment, well-siting, and sustainable groundwater management. Furthermore, the results are consistent with recent hydrogeophysical studies (Revil et al., 2024; Javed et al., 2024; Nugraha et al., 2025; Noorzamzarina et al., 2024) that emphasize the importance of combining ERI and IP methods for reliable characterization of complex subsurface environments.

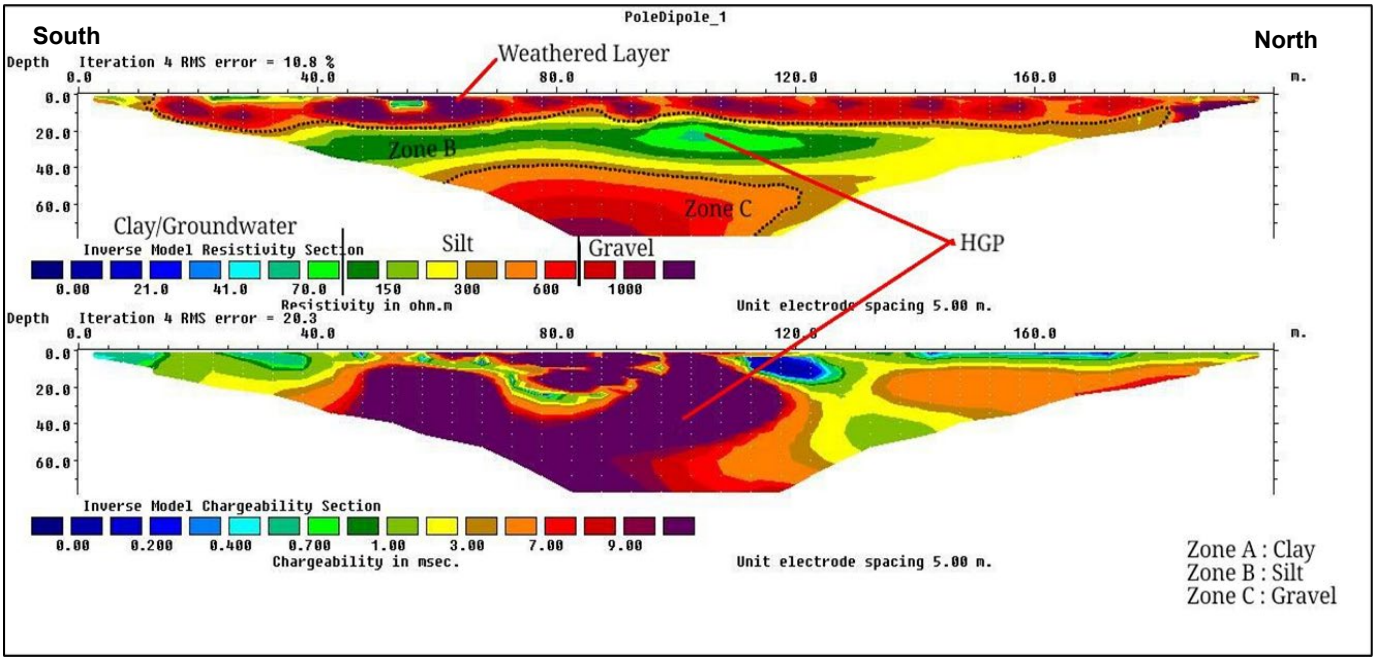

Figure 4: 2-D pseudosection profile for survey Line 3

4. CONCLUSION

This study demonstrates the effective application of Electrical Resistivity Imaging (ERI) in delineating groundwater-bearing zones to address local water supply challenges. By integrating both resistivity and chargeability

measurements, the investigation successfully identified subsurface features such as fractured and weathered bedrock zones, which are considered potential aquifers due to their enhanced secondary porosity and permeability. The resistivity and chargeability values obtained from the three survey lines—ranging from below 100 Ωm to 12 ms indicate the occurrence of saturated weathered zones and fractured formations that are conducive to groundwater accumulation. These anomalies correspond to areas where the contrast between conductive (saturated) and resistive (dry or compact) layers is well defined, signifying the capability of ERI to differentiate lithological variations with hydrogeological significance.

Furthermore, the ERI results provide a clearer understanding of the local geological and hydrogeological framework, emphasizing the spatial distribution of subsurface materials and their relationship to groundwater occurrence. This information is particularly valuable for guiding borehole siting, optimizing groundwater abstraction, and minimizing the risk of unsuccessful drilling. The findings also contribute to more informed decision-making in sustainable groundwater management and land-use planning, especially in regions characterized by heterogeneous and complex subsurface conditions. Overall, the integration of geophysical techniques, particularly the ERI method, has proven to be a cost-effective, non-invasive, and environmentally responsible approach to groundwater exploration. The results reaffirm the reliability of ERI as a diagnostic tool for assessing subsurface conditions and enhancing the understanding of groundwater potential, which is essential for the long-term management of water resources in the study area and similar geological settings.

ACKNOWLEDGEMENT

The authors express their sincere appreciation to Encik Mohd Khairul Aizuddin bin Razali for his valuable technical assistance. All individuals who contributed to this research are duly acknowledged for their significant efforts and active participation.

REFERENCES

Abdul Nassir, S., Loke, M.H., Lee, C. Y., Nawawi, M. N. M. (2000). Salt-water intrusion mapping by geoelectrical imaging surveys. Geophysical Prospecting, 48, 647–661. https://doi.org/10.1046/j.1365-2478.2000.00209.x

Abdullah, F.M., Loke, M.H., Nawawi, M., Abdullah, K., Younis, A., Arisona, A. (2022). Utilizing NWCR optimized arrays for 2D ERT survey to identify subsurface structures at Penang Island, Malaysia. Journal of Applied Geophysic, 196, 104518. https://doi.org/10.1016/j.jappgeo.2021.104518

Acworth, I. (2001). The electrical image method compared with resistivity sounding and electromagnetic profiling for investigation in areas of complex geology: A case study from groundwater investigation in a weathered crystalline rock environment. Exploration Geophysics, 32(2), 119-128. https://doi.org/10.1071/EG01119

Adeeko, T. O., Nordiana, M. M. (2018). Utilizing 2-D electrical resistivity imaging (ERI) to investigate groundwater potential. European Journal of Electrical Engineering, 20(1), 23-34. https://doi.org/10.3166/EJEE.20.23-34

Akhtar, N., Mislan, M. S., Syakir, M. I., Anees, M. T., Yusuff, M. S. M. (2021). Characterization of aquifer system using electrical resistivity tomography (ERT) and induced polarisation (IP) techniques. In IOP Conference Series: Earth and Environmental Science (Vol. 880, No. 1, p. 012025). IOP Publishing. https://iopscience.iop.org/article/10.1088/1755-1315/880/1/012025/pdf

Al-Khafaji, W. M. S. (2023). Methods in Geophysical Data Interpretation. Ph.D. Dissertation, Al-Karkh University of Science. Iraq.

As'ari, A., Herlina, J. T., & Gani, E. (2024). Detection of aquifer infiltration zones using resistivity and induced polarization methods. *Jurnal Ilmiah Sains*, 24(2), 1–10. https://doi.org/10.35799/jis.v24i2.58413

Azhar, A. T. S., Hazreek, Z. A. M., Aziman, M., Haimi, D. S., Hafiz, Z. M. (2016). Acidic barren slope profiling using electrical resistivity imaging (ERI) at Ayer Hitam area Johor, Malaysia. Journal of Physics: Conference Series, 710(012008), 1–10. https://iopscience.iop.org/article/10.1088/1742-6596/710/1/012008/pdf

Azhar, M., Suryadi, A., Samsudin, A. R., Yaacob, W. Z. W., Saidin, A. N. (2016). 2D geo-electrical resistivity imaging (ERI) of hydrocarbon contaminated soil. EJGE (Electron. J. Geotech. Eng), 21:299–304.

Azizan, F. A., Sah, S. S., Nawawi, M. M. (2018). Validation of groundwater potential zone based on imaging profiles using different array and lines of survey position. In IOP Conference Series: Materials Science and Engineering Vol. 429, No. 1, p. 012027). IOP Publishing. https://iopscience.iop.org/article/10.1088/1757-899X/429/1/012027/pdf

Batayneh, A. T. (2006). Use of electrical resistivity methods for detecting subsurface fresh and saline water and delineating their interfacial configuration: a case study of the eastern Dead Sea coastal aquifers, Jordan. Hydrogeology Journal, 14(7), 1277-1283. https://doi.org/10.1007/s10040-006-0034-3

Chambers, J.E., Gunn, D.A., Wilkinson, P.B., Meldrum, P.I., Haslam, E., Holyoake, S., Kirkham, M., Kuras, O., Merritt, A., Wragg, J. (2014). 4D electrical resistivity tomography monitoring of soil moisture dynamics in an operational railway embankment. Near Surf. Geophys, 12, 61–72. Available from: https://doi.org/10.3997/1873-0604.2013002

Dor, N., Syafalni, S., Abustan, I., Rahman, M. T. A., Nazri, M. A. A., Mostafa, R., Mejus, L. (2011). Verification of surface-groundwater connectivity in an irrigation canal using geophysical, water balance and stable isotope approaches. Springer: Water Resources Management, 25(11), 2837–2853.

Ejije, C. E., Atakpo, E. A. (2025). Delineation of subsurface lithology and aquifer structures using electrical resistivity surveys in parts of Ukwuani Local Government Area of Delta State. Nigerian Journal of Science and Environment, 23(1), 61-67. https://www.ajol.info/index.php/njse/article/view/297176

Galazoulas, E. C., Mertzanides, Y. C., Petalas, C. P., Kargiotis, E. K. (2015). Large scale electrical resistivity tomography survey correlated to hydrogeological data for mapping groundwater salinization: a case study from a multilayered coastal aquifer in Rhodope, Northeastern Greece. Environmental processes, 2(1), 19-35. https://link.springer.com/article/10.1007/s40710-015-0061-y

Hazreek, Z. A. M., Nizam, Z. M., Aziman, M., Dan, M. M., Shaylinda, M. Z. N., Faizal, T. B. M., ... Alel, M. N. A. (2018). Mapping on slope seepage problem using electrical resistivity imaging (ERI). In Journal of Physics: Conference Series Vol. 995, No. 1, 012091. IOP Publishing. https://iopscience.iop.org/article/10.1088/1742-6596/995/1/012091/pdf

Islami, N., Irianti, M., Yusoff, I. (2024). An effective method for quantitative interpretation of seawater intrusion in shallow aquifers from electrical resistivity data. *Current Applied Science and Technology*, 25(1), e0261277. https://doi.org/10.55003/cast.2024.261277

Javed, U., Kumar, P., Hussain, S., Taufiq, N., Shah, F., Shahbaz, A., Karamat, A. (2024). Geospatial analysis of soil resistivity and hydro-parameters for groundwater assessment. *Discover Geoscience*, 2(3), 45. https://doi.org/10.1007/s44288-024-00004-6

Khan, A. A., Shuib, M. K. (2016). A Review of the Bentong-Raub Suture vis-à-vis New Insight of the Tectonic Evolution of Malay Peninsula, South East Asia. Acta Geologica Sinica-English Edition, 90(5), 1865-1886. https://onlinelibrary.wiley.com/doi/abs/10.1111/1755-6724.12822

Loke, M. H. (2002). Electrical Imaging Surveys for Environmental and Engineering Studies. A Practical Guide to 2-D and 3-D Imaging Surveys, 61.

Loke, M., Chambers, J., Ogilvy, R. (2006). Inversion of 2D spectral induced polarization imaging data. Geophys Prospect. 54, 287–301. https://doi.org/10.1111/j.1365-2478.2006.00537.x

Metcalfe, I. (2013). Tectonic evolution of the Malay Peninsula and Sundaland. *Gondwana Research*, 24(**1**), 32–60.

Noorzamzarina S., Alya, S. B., Nursufiah, S., Wani, S. U, Nor, S. S., Fazrul, R. S. (2023). Landslide investigation using Electrical Resistivity Imaging (ERI) method at Kg. Chuchoh Puteri, Kuala Krai, Kelantan, Malaysia. BIO Web of Conferences 73, 04003. https://doi.org/10.1051/bioconf/20237304003

Noorzamzarina S., Nur Azlin M. R., Nursufiah, S., Fazrul, R. S. (2024). Identification of potential groundwater sources using Electrical Resistivity Imaging (ERI) method in Jambu Lawar, Machang, Kelantan. BIO Web of Conferences 131, 04015. https://doi.org/10.1051/bioconf/202413104015

Nugraha, G. U., Bakti, H., Lubis, R. F., Mulyono, A., Ulfa, Y., Sudrajat, Y. (2025). Data-driven resistivity zonation integrating inversion kriging and clustering for

subsurface characterization in groundwater exploration. *Discover Water*, 5, 62. https://doi.org/10.1007/s43832-025-00261-7

Oyeyemi, K. D., Aizebeokhai, A. P., Attat, O. F. (2018). Evaluation of groundwater pollution near municipal solid waste landfill site using ERI technique: A case study in Southwestern Nigeria. Nature Environment and Pollution Technology, 17(2), 453-458. https://core.ac.uk/download/pdf/159129324.pdf

Petrick, N., Jubidi, M. F., Abir, I. A. (2023). Groundwater Potential Assessment of Penang Island, Malaysia Through Integration of Remote Sensing and GIS with Validation by 2D-ERT. Natural Resources Research, Vol. 32, No. 2, 523-541. https://doi.org/10.1007/s11053-023-10164-w

Rajendran, G., Mohammed, M., Shivakumar, S., Merera, W., Taddese, K. (2020). Geospatial techniques amalgamated with two-dimensional electrical resistivity imaging for delineation of groundwater potential zones in West Guji Zone, Ethiopia. Groundwater for Sustainable Development, 11, 100407. https://www.sciencedirect.com/science/article/pii/S2352801X2030031X

Revil, A., Peyras, L., Vaudelet, P. (2024). Groundwater flow paths using combined self-potential, electrical resistivity, and induced polarization signals. Geophysical Journal International, 239(2), 798–820. https://doi.org/10.1093/gji/ggae291

Riwayat, A. I., Nazri, M. A. A., Abidin, M. H. Z. (2018). Application of electrical resistivity method (ERM) in groundwater exploration. In Journal of Physics: Conference Series (Vol. 995, No. 1, p. 012094). IOP Publishing. https://iopscience.iop.org/article/10.1088/1742-6596/995/1/012094/meta

Riwayat, A. I., Nazri, M. A. A., Ahmad, N. A. (2022). Mapping of Potential Groundwater Using Electrical Resistivity Imaging (ERI) at Low Land Area of Parit Raja Johor. International Journal of Integrated Engineering, 14(9), 15-23. https://publisher.uthm.edu.my/ojs/index.php/ijie/article/view/11412

Saad, R., Nawawi, M. N. M., Mohamad, E. T. (2012). Groundwater detection in alluvium using 2-D electrical resistivity tomography (ERT). Electron. J. Geotech. Eng, 17.

Samsudin, A. R. (2010). Utilizations of geophysical methods in hydrogeology. Conference: Groundwater in the context of IWRM. Available from: https://www.researchgate.net/publication/296701449

Soekarno, I. et al. (2024). A Methodology for Water Resource Management and the Pre-feasibility Study of Coastal Reservoirs in Indonesia. Water, 16(2),344.

Suryadi, A., Batara, A., N., S. (2019). Electrical resistivity imaging (ERI) and induced polarization (IP) survey to solve water drought problem at Alor Gajah. Melaka, Malaysia. IOP Conf. Ser. Mater. Sci. Eng. 532, 532:012025.

Vaudelet, P., Schmutz, M., Pessel, M., Franceschi, M., Guerin, R., Atteia, O., Bégassat, P. (2011). Mapping of contaminant plumes with geoelectrical methods. A case study in urban context. Journal of Applied Geophysics, 75(4), 738-751. https://www.sciencedirect.com/science/article/pii/S0926985111002230

